

Influence of Sensor Feedback Limitations on Power Oscillation Damping and Transient Stability

Joakim Björk, Danilo Obradović, Karl Henrik Johansson
KTH Royal Institute of Technology, Stockholm, Sweden
joakbj@kth.se, daniloo@kth.se, kallej@kth.se

Lennart Harnefors
ABB Corporate Research, Västerås, Sweden
lennart.harnefors@se.abb.com

Abstract—In this work, fundamental sensor feedback limitations, using a linear controller with local frequency measurement, are considered. It is shown that improved damping of inter-area oscillations must come at the cost of reduced transient stability margins, regardless of control design. The results are verified in the Kundur four-machine two-area test system.

Index Terms—Fundamental limitations, inter-area oscillations, power oscillation damping, sensor feedback, transient stability.

I. INTRODUCTION

With a steadily growing demand, deregulated market, and rising share of renewables, long-distance power transfers are increasing. In heavily stressed grids, poorly damped inter-area modes are a greater concern [1]. An example is the western North American blackout of August 10, 1996, resulting from the instability of a 0.25 Hz inter-area mode [2]. To improve stability margins, and thereby increasing the transmission capacity, power oscillation damping (POD) control is normally implemented. Typical actuators are the excitation systems of generators via power system stabilizers (PSSs) [3]–[5], and power electronic devices such as high-voltage dc (HVDC) links, flexible ac transmission system devices, and inverter based power production [6]–[14].

In [6], the damping of a 0.4 Hz inter-area mode in the Hydro-Québec grid is studied. It is found that damping control based on specific local measurements may cause transient instability for some contingencies whereas wide-area measurements yield transient stability improvements as well as damping over a wide range of operating conditions. Stability issues are often caused by a combination of dynamical properties. Because of this, traditional damping control are often tuned conservatively to guarantee overall system stability [5].

In [7] active power modulation of the Pacific HVDC Inertia is considered in the western North American power system. Local frequency measurement is found as a suitable measurement signal for POD as it shows good observability

and robust performance over a range of operating conditions. However, it is observed that damping based on local frequency measurements may deteriorate transient performance and cause first swing instability for some scenarios. In [8], the authors study control limitations due to indirect measurement of the signal to be controlled. Trade-offs between local measurements and external wide-area measurement, with possible communication delays, are studied explicitly in a general control configuration. In this work, the constraints imposed by a sensor feedback controller using local frequency are analyzed to give insight into the fundamental limitations of this control problem. Performance issues may be caused by the choice of measurements, but may also be a consequence of the control design. With optimization based control design, improved performance can often be achieved [15]–[17].

However, satisfactory tuning of optimization criteria can be an endless task as evaluating the achieved closed-loop performance is often far from trivial. Fundamental design limitations helps us to understand if unsatisfactory closed-loop performance—be it with traditional or optimization based control design—are due to the engineer not specifying the correct design criteria, or due to inherent system limitations.

The contribution of this work is to analyze the fundamental limitations for improving the overall stability of the power system using local frequency measurements. The sensor feedback problem is partitioned into a control and filtering problem to distinguish between control limitations and filtering limitations imposed by indirect measurement. Using integral constraints, it is shown that any damping improvement based on local frequency measurements, must come at the cost of reduced transient stability margins.

The remainder of this paper is organized as follows. In Section II a linearized power system model is derived. Section III introduces linear control and filtering theory. In Section IV fundamental sensor feedback limitations are derived and in Section V the result are verified on a detailed nonlinear power system model. Section VI concludes the work.

II. TWO-MACHINE POWER SYSTEM

Let system voltages be given by the complex vector

$$U/\varphi^T = [U_1/\varphi_1, U_2/\varphi_2, \dots, U_N/\varphi_N] = [E'_q/\delta^T, V/\theta^T],$$

where the vectors E'_q and $\delta \in \mathbb{R}^{n_\delta}$ represent the internal voltage amplitudes and phase angles of the machines and V

This work was done under the PhD program in the digitalization of electric power engineering, School of Electrical Engineering and Computer Science, KTH Royal Institute of Technology, Sweden.

The work was supported in part by the Knut and Alice Wallenberg Foundation, the Swedish Research Council, the Swedish Foundation for Strategic Research, and by the multiDC project, funded by Innovation Fund Denmark, Grant Agreement No. 6154-00020B.

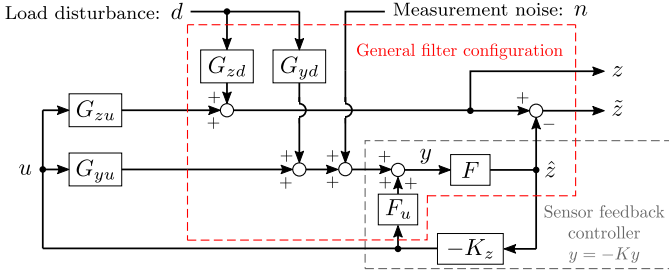


Fig. 3. General control configuration as a control and filtering problem. The filter F_u is assumed to decouple the control input u from the estimation error \tilde{z} . Note that the sensor feedback controller $K = (1 + K_z F F_u)^{-1} K_z F$.

Let the scalar transfer function G_{yu} represent a plant with output y and input u . Consider a linear controller $u = -Ky$ where K is any proper rational transfer function.

Definition 1 (Sensitivity functions): The closed-loop sensitivity and complementary sensitivity functions are given by

$$\mathcal{S} = (1 + G_{yu}K)^{-1}, \quad \text{and} \quad \mathcal{T} = 1 - \mathcal{S}, \quad \text{respectively.}$$

Lemma 1 (Interpolation constraints [19]): For internal stability, no cancellation of open right half plane (ORHP) poles or zeros are allowed between the plant and the controller. Let $\{p_i: i = 1, \dots, n_p\}$ and $\{q_i: i = 1, \dots, n_q\}$ be the ORHP poles and zeros of the plant G_{yu} . Then for all p_i and q_i ,

$$\begin{aligned} \mathcal{S}(p_i) &= 0, & \mathcal{T}(p_i) &= 1, \\ \mathcal{S}(q_i) &= 1, & \mathcal{T}(q_i) &= 0. \end{aligned}$$

Since \mathcal{S} and \mathcal{T} represent closed-loop amplification of load disturbances and measurement noise, respectively. The interpolation constraints limits the achievable performance.

Lemma 2 (Bode integral [19]): Suppose that the loop-gain $G_{yu}K$ is a proper rational function. Then, if $\mathcal{S}(\infty) = \mathcal{S}_\infty \neq 0$

$$\int_0^\infty \ln \left| \frac{\mathcal{S}(j\omega)}{\mathcal{S}_\infty} \right| d\omega = \frac{\pi}{2} \lim_{s \rightarrow \infty} \frac{s[\mathcal{S}(s) - \mathcal{S}_\infty]}{\mathcal{S}_\infty} + \pi \sum_{i=1}^{n_p} p_i. \quad (9)$$

Typically, both G_{yu} and K are strictly proper and thus the limit on the right hand side of (9) goes to 0. The integral (9) then dictates that any frequency range with disturbance attenuation $|\mathcal{S}(j\omega)| < 1$ need to be balanced with an equally large region with disturbance amplification $|\mathcal{S}(j\omega)| > 1$, plus the contribution from any ORHP poles in G_{yu} [15].

In general the measured output y differs from the performance variable z that we want to control. For an open-loop plant in the general control configuration shown in Fig. 3, the goal is to design a sensor feedback controller K that reduces the amplitude of the closed-loop system from d to z

$$\mathcal{T}_{zd} = G_{zd} - G_{zu}K(1 + G_{yu}K)^{-1}G_{yd}. \quad (10)$$

In the general control configuration, ORHP in G_{yd} , G_{zd} , and G_{zu} may put further restrictions on achievable performance [20]. The general control problem can be separated into a control and estimation problem as shown in Fig. 3. This work focuses on the latter by studying limitations in the linear scalar filtering problem.

Assume that the system is detectable from y , i.e, all unobservable states are stable, and that $\hat{z} = Fy$ is an unbiased, bounded error estimate of z . An observer is a bounded error estimator if for all finite initial states, the estimation error $\tilde{z} = z - \hat{z}$ is bounded for all bounded inputs. A bounded error estimator is unbiased if u is decoupled from \tilde{z} [19].

Definition 2 (Filtering sensitivity functions [19]): If G_{yd} is detectable, F is a stable filter, and G_{zd}^{-1} is right invertible¹, the filtering sensitivity functions are given by

$$\mathcal{P} = (G_{zd} - FG_{yd})G_{zd}^{-1}, \quad \text{and} \quad \mathcal{M} = FG_{yd}G_{zd}^{-1}, \quad (11)$$

with $\mathcal{P} + \mathcal{M} = 1$ at any $s \in \mathbb{C}$ that is not a pole of \mathcal{P} or \mathcal{M} .

The filtering sensitivity function \mathcal{P} represent the relative effect of disturbances d on the estimation error \tilde{z} , while the complementary filter sensitivity \mathcal{M} represent the relative effect of d on the estimate \hat{z} .

Lemma 3 (Interpolation constraints on \mathcal{P} and \mathcal{M} [19]): Let $\{\rho_i: i = 1, \dots, n_\rho\}$ be the ORHP poles of G_{zd} and let $\{\xi_i: i = 1, \dots, n_\xi\}$ be the ORHP zeros of G_{yd} that are not also zeros of G_{zd} . Assume that F is a bounded error estimator. Then

$$\begin{aligned} \mathcal{P}(\rho_i) &= 0, & \mathcal{M}(\rho_i) &= 1, \\ \mathcal{P}(\xi_i) &= 1, & \mathcal{M}(\xi_i) &= 0. \end{aligned}$$

Lemma 4 (Bode integral for \mathcal{P} [19]): Suppose that \mathcal{P} is proper and that F is a bounded error estimate. Let the ORHP zeros of \mathcal{P} be $\{\rho_i: i = 1, \dots, n_\rho\}$ and let $\{\zeta_i: i = 1, \dots, n_\zeta\}$ be the ORHP zeros of G_{zd} such that $F(\zeta_i)G_{yd}(\zeta_i) \neq 0$. Then if $\mathcal{P}(\infty) = \mathcal{P}_\infty \neq 0$

$$\int_0^\infty \ln \left| \frac{\mathcal{P}(j\omega)}{\mathcal{P}_\infty} \right| d\omega = \frac{\pi}{2} \lim_{s \rightarrow \infty} \frac{s[\mathcal{P}(s) - \mathcal{P}_\infty]}{\mathcal{P}_\infty} + \pi \sum_{i=1}^{n_\rho} \rho_i - \pi \sum_{i=1}^{n_\zeta} \zeta_i. \quad (12)$$

Similar to Lemmas 1 and 2, this tells us that the estimation error cannot be made arbitrarily small over all frequencies.

IV. SENSOR FEEDBACK LIMITATIONS

In this section, limitations for damping control based on local phase angle or frequency measurements are presented.

A. External Measurement $y = \omega_1 - \omega_2$

Inter-area oscillations are a electromechanical phenomena where groups of machines in one end of the system swing against machines in the other end of the system [3]. Consider the two-machine system shown in Figs. 1 and 2. Here, the inter-area mode can be represented by the relative frequency

$$z = s(\delta_1 - \delta_2) = \omega_1 - \omega_2. \quad (13)$$

If available, $y = z$ is an ideal feedback signal [14]. With input-output mappings given by the transfer function matrix in (6) the system to stabilize with feedback control becomes

$$G_{zu} = \frac{X_1^* - X_2^*}{MX_\Sigma^*} \frac{s}{s^2 + \Omega^2}. \quad (14)$$

¹For G_{zd} to be right invertible there need to be at least as many inputs as signals to be estimated. Note that G_{zd}^{-1} is not necessarily proper.

Lemma 5: Suppose that $y = z$, G_{zu} have no ORHP zeros, and that $|G_{zd}|$ roll off at higher frequencies. Then for every positive ϵ there exist a controller K such that

$$|\mathcal{T}_{zd}(j\omega)| < \epsilon, \forall \omega. \quad (15)$$

Proof: First we note that since z is available for feedback, we directly have $u = -Ky = -Kz$. Thus the closed-loop system (10) reduces to $\mathcal{T}_{zd} = \mathcal{S}G_{zd}$. Since $|\mathcal{T}_{zd}| \leq |\mathcal{S}||G_{zd}|$, (15) is fulfilled if

$$|\mathcal{S}(j\omega)| < \epsilon/|G_{zd}(j\omega)|, \forall \omega.$$

If there are no ORHP zero in G_{zu} then, by Lemma 1, \mathcal{S} is not constrained at any specific frequencies. If KG_{zu} has relative degree ≤ 1 , then \mathcal{S} can theoretically be made arbitrarily small over all frequencies.

If KG_{zu} has relative degree ≥ 2 then the frequency range where $|\mathcal{S}| < 1$ has to be compensated with a range where $|\mathcal{S}| > 1$. However, since there are no ORHP zeros limiting the closed-loop bandwidth, $|\mathcal{S}| > 1$ can be chosen for higher frequencies where $|G_{zd}|$ is sufficiently small. ■

Lemma 5 implies that a controller can be designed so that excitation of the inter-area mode, by load disturbances, can be made arbitrarily small if enough input power is available.

Example 1: Suppose that we choose proportional control $u = -kz$ then with G_{zu} given by (14)

$$\mathcal{S} = \frac{s^2 + \Omega^2}{s^2 + sk \frac{X_1^* - X_2^*}{MX_\Sigma^*} + \Omega^2}.$$

By Lemma 2 we then have, for $\text{sgn } k = \text{sgn}(X_1^* - X_2^*)$,

$$\int_0^\infty \ln |\mathcal{S}(j\omega)| d\omega = \frac{\pi}{2} \lim_{s \rightarrow \infty} s [\mathcal{S}(s) - 1] = -k \frac{\pi}{2} \frac{X_1^* - X_2^*}{MX_\Sigma^*}$$

which, for $|k| > 0$, is always < 0 .

B. Local Measurement $y = \theta$ —Filtering Limitations

Typically the industry is restrained from using external communication for crucial system functions such as POD. Thus, using relative frequency difference for feedback is normally not an option. The controller instead need to rely on local measurements.

Using an inverse based controller we can make the sensitivity arbitrarily small as in Lemma 5. The difference however, is that making \mathcal{S} small is not necessarily the same as making the closed-loop system (10) small if $y \neq z$.

Consider the two machine system shown in Fig. 1 using local phase angle measurement, $y = \theta$. With input-output mappings given by (6) to (8)

$$\begin{bmatrix} G_{zd1} & G_{zd2} \\ G_{yd1} & G_{yd2} \end{bmatrix} = G_0 \begin{bmatrix} s^3 & -s^3 \\ \frac{X_2^*}{X_\Sigma^*} \left(s^2 + \frac{1}{MX_2^*} \right) & \frac{X_1^*}{X_\Sigma^*} \left(s^2 + \frac{1}{MX_1^*} \right) \end{bmatrix}. \quad (16)$$

Assume that $0 \leq X_1^* < X_2^* \leq X_\Sigma^*$, i.e., machine 1 is closest to the measurement bus. Then the corresponding complex conjugated zero pairs q_1 and q_2 fulfill

$$|q_1| = 1/\sqrt{MX_2^*} < |q_2| = 1/\sqrt{MX_1^*}.$$

Partition the general control problem (10) into a control and an estimation problem as shown in Fig. 3. Lemma 5 implies that any limitations on the closed-loop system will be linked to limitations in the observer. Assume that the observer is an unbiased, bounded error estimator. Limitations in the nominal system are then given by the filtering sensitivity functions (11).

Lemma 6: Suppose that $y = \theta$ and let \mathcal{P}_1 and \mathcal{P}_2 be the filtering sensitivity functions associated with d_1 and d_2 respectively. Then an estimator $\hat{z} = Fy$, such that

$$\max(|\mathcal{P}_1(j\omega)|, |\mathcal{P}_2(j\omega)|) < 1$$

is only possible for the frequency interval $\omega \in [|q_1|, |q_2|]$.

Proof: The complementary filter sensitivity \mathcal{M} represent the relative effect of disturbances d on the estimate \hat{z} , while the filtering sensitivity \mathcal{P} represent the relative effect of disturbances d on the estimation error $\tilde{z} = z - \hat{z}$. Thus, a minimum requirement for $|\mathcal{P}| < 1$ is that the estimate \hat{z} has the same sign as z , i.e., $\mathcal{M} > 0$.

With (16) the complementary filtering sensitivity functions to consider becomes

$$\begin{aligned} \mathcal{M}_1 &= FG_{yd1}G_{zd1}^{-1} = -F \frac{X_2^*}{X_\Sigma^*} \frac{s^2 + 1/MX_2^*}{s^3}, \\ \mathcal{M}_2 &= FG_{yd2}G_{zd2}^{-1} = F \frac{X_1^*}{X_\Sigma^*} \frac{s^2 + 1/MX_1^*}{s^3}. \end{aligned} \quad (17)$$

Thus, it is clear that $\mathcal{M}_1(j\omega), \mathcal{M}_2(j\omega) > 0$ is only possible for $\omega \in [\sqrt{1/MX_2^*}, \sqrt{1/MX_1^*}] = [|q_1|, |q_2|]$. ■

Example 2 (Filtering limitations): Consider a two-machine power system as shown in Fig. 1 with linear dynamics (16) given by Section II. Let the line reactance $X_\Sigma^* = 1$ p.u. and scale the machine inertia M so that the inter-area modal frequency $\Omega = \sqrt{2/MX_\Sigma^*} = 1$ rad/s. In addition, add a 0.05 p.u./rad/s damping constant at each machine so that the inter-area mode has small but positive damping.²

Fig. 4 shows the Bode diagram of $G_{yd1}G_{zd1}^{-1}$ and $G_{yd2}G_{zd2}^{-1}$. These represent the complementary filtering sensitivity functions (17) with the filter yet to be designed. To understand the implications of Lemma 6, consider two extreme cases.

First, consider the case shown in Fig. 4 where the control bus is located close to machine 1 with $X_1^* = 0.1$ p.u. and $X_2^* = 0.9$ p.u. Note that as $X_1^* \rightarrow 0$, $|q_1| \rightarrow \Omega/\sqrt{2}$ and $|q_2| \rightarrow \infty$. To improve closed-loop performance in the presence of disturbances, a good estimate of z is required where $|G_{zd1}|$ ($= |G_{zd2}|$) is large. As seen in Fig. 4, $|G_{zd1}(j\omega)|$ peaks at $\omega = \Omega$ and then rolls off for lower and higher frequencies. To keep the estimation error small, accurate estimation is also required for frequencies where $G_{yd1}G_{zd1}^{-1}$ and $G_{yd2}G_{zd2}^{-1}$ are large. For closed-loop performance, this implies that the estimation error at lower frequencies is of greater interest.

Assume that F is designed so that $\mathcal{M}_1(j\omega) \approx 1 \forall \omega$. Following the numbers listed in Fig. 4:

²If we introduce damping in the system, poles (7) and zeros (8) will move into the open left half plane (OLHP). With a higher order model (3) that also involve voltage dynamics, zeros may very well move into the ORHP. However, the studied limitation applies to both ORHP and OLHP zeros.

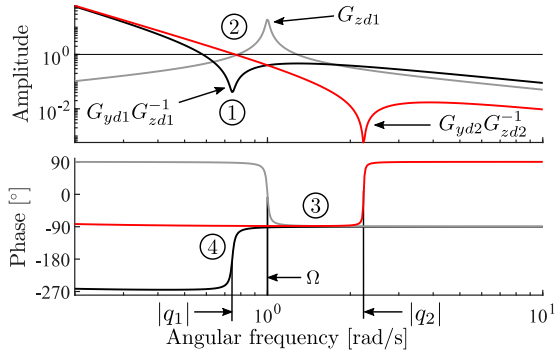


Fig. 4. Bode diagrams that visualize the limitations of using local phase angle measurement $y = \theta$ in Example 2.

- ① The complex conjugated zero, q_1 , is canceled by F making $\mathcal{M}_1 = FG_{yd1}G_{zd1}^{-1} \rightarrow 1$ at $\omega = |q_1|$.
- ② Cancellation occurs at a point where $|G_{yd2}G_{zd2}^{-1}|$ is large.
- ③ In a bandwidth around the modal frequency Ω both transfer functions have the same phase. Thus $\mathcal{M}_1, \mathcal{M}_2 > 0$ can be guaranteed no matter the origin of the disturbance.
- ④ At $\omega = |q_1|$ the phase difference between $G_{yd1}G_{zd1}^{-1}$ and $G_{yd2}G_{zd2}^{-1}$ changes sign. Thus the estimate for disturbances from one end of the system will have an incorrect sign. With cancellation of q_1 at ① this results in a large \mathcal{M}_2 with incorrect sign and thus the disturbance response from d_2 will be amplified.

Second, consider the case where the control bus is located in the electrical midpoint between the two machines. In this case $|q_1| = |q_2| = \Omega$ and the frequency window ③ where both d_1 and d_2 can be attenuated disappears. This is reasonable since the inter-area mode is unobservable from phase measurement at the electrical midpoint [12].

C. Local Measurement $y = \theta$ —Feedback Limitations

The aim of a feedback controller is to reduce the amplitude of the closed-loop system (10) compared to the open-loop system, i.e., make $|\mathcal{T}_{zd}| < |G_{zd}|$. Multiplying with G_{zd}^{-1} this can be expressed using the disturbance response ratio [20]

$$|\mathcal{R}_{zd}| = |1 - G_{zu}K(1 + G_{yu}K)^{-1}G_{yd}G_{zd}^{-1}| < 1.$$

Lemma 7: Suppose $y = \theta$ and let \mathcal{R}_{zd1} and \mathcal{R}_{zd2} be the disturbance response ratios associated with d_1 and d_2 respectively. Then a sensor feedback controller $u = -Ky$, such that

$$\max(|\mathcal{R}_{zd1}(j\omega)|, |\mathcal{R}_{zd2}(j\omega)|) < 1, \quad (18)$$

is only possible for the frequency interval $\omega \in [|q_1|, |q_2|]$.

Proof: Follows from Lemma 6. ■

Theorem 1: Suppose that $y = \theta$ and that a sensor feedback controller $u = -Ky$ achieves disturbance attenuation (18) in the interval $\omega \in [|q_1|, |q_2|]$. Then disturbance amplification

$$\max(|\mathcal{R}_{zd1}(j\omega)|, |\mathcal{R}_{zd2}(j\omega)|) > 1,$$

is unavoidable in frequency intervals $\omega < |q_1|$ and $|q_2| < \omega$.

Proof: Since any practical filter is strictly proper, \mathcal{M}_1 and \mathcal{M}_2 in (17) have relative degrees ≥ 2 .

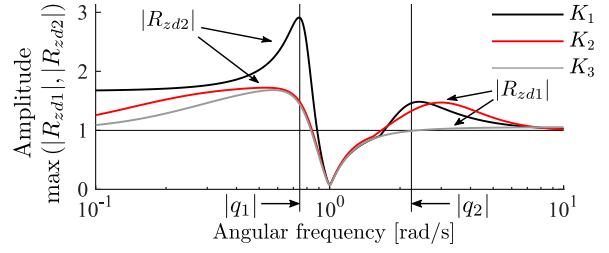


Fig. 5. Disturbance response ratios with feedback from local phase angle measurement $y = \theta$ in Example 3.

Write $\{\mathcal{M}_k : k = 1, 2\}$ as the polynomial fraction

$$\mathcal{M}_k(s) = \frac{\alpha(s)}{\beta(s)} = \frac{\alpha_0 + s\alpha_1 + \dots + s^{n_\alpha}\alpha_{n_\alpha}}{\beta_0 + s\beta_1 + \dots + s^{n_\beta}\beta_{n_\beta}},$$

and $\mathcal{P}_k(s) = 1 - \mathcal{M}_k(s) = (\beta(s) - \alpha(s))/\beta(s)$. With $n_\beta - n_\alpha \geq 2$, $\mathcal{P}_k(\infty) = 1$, and the Bode integral constraint (12)

$$\begin{aligned} \int_0^\infty \ln |\mathcal{P}_k(j\omega)| d\omega &= \frac{\pi}{2} \lim_{s \rightarrow \infty} s [\mathcal{P}_k(s) - 1] + \pi \sum_{i=1}^{n_\theta} \varrho_i \\ &= \frac{\pi}{2} \lim_{s \rightarrow \infty} -s\mathcal{M}_k(s) + \pi \sum_{i=1}^{n_\theta} \varrho_i = \pi \sum_{i=1}^{n_\theta} \varrho_i \geq 0, \end{aligned}$$

where ϱ_i are any eventual ORHP zeros in \mathcal{P}_k . Thus, by Lemma 4, any region with $|\mathcal{P}_k(j\omega)| < 1$ need to be compensated with an (at least) equally large region with $|\mathcal{P}_k(j\omega)| > 1$. From Lemma 6 it then follows that

$$\max(|\mathcal{P}_1(j\omega)|, |\mathcal{P}_2(j\omega)|) > 1,$$

and thus, from Lemma 7, disturbance amplification

$$\max(|\mathcal{R}_{zd1}(j\omega)|, |\mathcal{R}_{zd2}(j\omega)|) > 1,$$

is unavoidable in the intervals $\omega < |q_1|$ and $|q_2| < \omega$. ■

The proposed sensor feedback limitations does not require the computation of the controller. But for illustrative purposes this is of course needed. In practice, POD is typically implemented as a proportional controller with the required phase compensation to improve damping [3]. Since this design is fairly limited, dynamical controllers designed using \mathcal{H}_2 optimization will also be considered in the following example.

Example 3 (Feedback limitations): Consider the two-machine power system introduced in Example 2. Limitations on the disturbance response ratio $\max(|\mathcal{R}_{zd1}|, |\mathcal{R}_{zd2}|)$ are shown in Fig. 5 using three controllers $\{K_i : i = 1, 2, 3\}$.

Controllers K_2 and K_3 are tuned to minimize the \mathcal{H}_2 norm of the close-loop plant in Fig. 3, between load disturbances d and measurement noise n , and the weighted performance output z and input u . The performance weight [15] W_z are used to trade-off between performance and input usage.

K_1) Proportional controller with 90° phase compensation

$$K_1 = ks \frac{10\Omega}{s + 10\Omega}, \quad k = 0.2 \text{ p.u./rad.}$$

K_2) Moderate \mathcal{H}_2 controller tuned with performance weight $W_z = 10$. External inputs are modeled as white noise with amplitudes $|d_1|, |d_2| = 1$ p.u. and $|n| = 0.05$ rad.

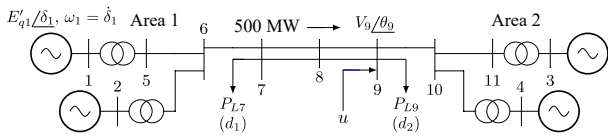


Fig. 6. Four-machine two-area system [3], [21]. Modifications: inertia reduced to 75%, inter-area power flow increased to 500 MW, and PSSs tuned down for a marginally damped inter-area mode.

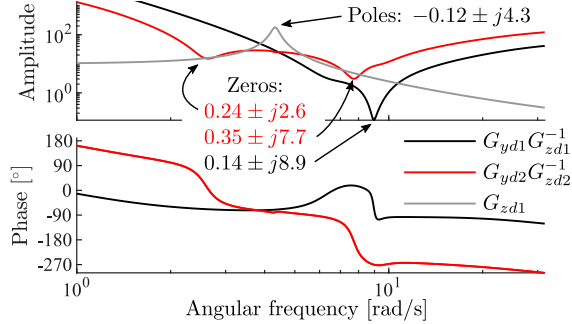


Fig. 7. Bode diagrams that visualize the sensor feedback limitations with input and output according to Fig. 6. The close resemblance to Fig. 4 validates the analysis in Section IV.

K_3) Aggressive \mathcal{H}_2 controller with $W_z \rightarrow \infty$ and $|n| \rightarrow 0$.

To avoid input usage at steady state, a wash-out filter [3] with a 5 s time constant is also implemented for all controllers.

In Fig. 5, the maximum disturbance response ratio is shown. As stated in Lemma 7, $\max(|\mathcal{R}_{zd1}(j\omega)|, |\mathcal{R}_{zd2}(j\omega)|) < 1$ is only achievable for $\omega \in [|q_1|, |q_2|]$ and in accordance with Theorem 1, disturbance amplification is unavoidable outside of $\omega \in [|q_1|, |q_2|]$. As discussed in Example 2 the disturbance amplification is worse for angular frequencies around the low frequency zero $|q_1|$.

V. SIMULATION STUDY

In this section, the influence of sensor feedback limitations are shown for a detailed nonlinear power system model. The considered system is the Kundur four-machine two-area test system [3] shown in Fig. 6. For illustrative purposes, the system—from Simulink implementation in [21]—have been modified to reduce stability margins.

A. Filtering Limitations

To represent the inter-area mode, the performance variable z is chosen as the states projected on the corresponding left eigenvector pair. As the inter-area mode is dominated by electromechanical dynamics, this is roughly equivalent to (13) even though more dynamics have been introduced [13].

The sensor feedback limitations using $y = \theta_9$ are shown Fig. 7. The bode diagram bares close resemblance to the simplified model in Fig. 4. The main difference is that $G_{yd2}G_{zd2}^{-1}$ shows a prominent zero also at higher frequencies. This can be expected as d_2 is at the control bus and should therefore, according to (6), show both zero pairs. For the integrity of the system, low frequency amplifications are of greater concern.

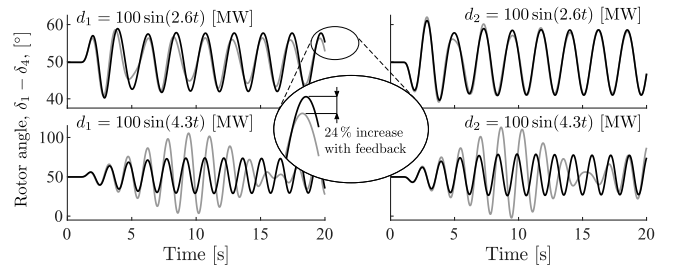


Fig. 8. Rotor phase angles differences following sinusoidal load disturbances d_1 and d_2 at buses 7 and 9 respectively. The black (gray) lines are the resulting rotor phase angle difference with (without) feedback control, using $y = \theta_9$.

B. Closed-Loop Frequency Response

An \mathcal{H}_2 optimal controller is implemented to improve damping of the inter-area mode using local phase angle measurement and active power injections at bus 9. The POD controller is tuned to improve damping from 2.7% to 10%. By Theorem 1 we would expect the controller to amplify load disturbances from one end of the system. The breaking point is the low frequency (complex conjugated) zero pair that are associated with disturbances closer to the measurement bus. In Fig. 7 we see that this corresponds to a (RHP) zero pair at roughly 2.6 rad/s. As can be seen, disturbances with an angular frequency of 4.3 rad/s are well damped both from bus 7 in Area 1 and from bus 9 in Area 2.

Remark 2: Large sinusoidal disturbances with a 100 MW amplitude are considered. This result in a large shift from the initial linearization point. Yet, nonlinear simulation shows the results expected from the linear analysis.

For internal stability, Lemma 1 tells us that $S = 1$ at any ORHP zero of G_{yu} . In this case $G_{yu} = G_{yd2}$ and therefore we have RHP zeros in $0.24 \pm j2.6$ rad/s. Thus we would expect that the closed-loop disturbance response is next to unchanged for d_2 at 2.6 rad/s. Looking at the top-right graph in Fig. 8 we see that this is indeed the case. However, by Theorem 1 we also have that at least one of the disturbances need to be amplified for angular frequencies < 2.6 rad/s. In the top-left graph in Fig. 8 we see that the implemented controller amplifies low-frequency disturbances from d_1 .

C. Closed-Loop Transient Stability

The amplification of disturbances shown in Fig. 8 may seem insignificant. However, for a system operated close to its stability limit this can have implications for transient stability. A large phase angle difference between the two areas may cause a separation in the system due to the nonlinear electrical dynamics. Therefore, it is crucial that $|z|$ is kept small.

In Fig. 9, the system response to a 1 s, 350 MW disturbance step is shown. Worst case disturbances are those that increase the rotor phase angle difference. Therefore we consider a load loss at bus 5 and a generation loss at bus 11 (simulated as active power loads). This could for example represent the commutation failure of an exporting or importing HVDC link. As seen in Fig. 9, both the damping and transient response are improved for disturbances occurring close to the control

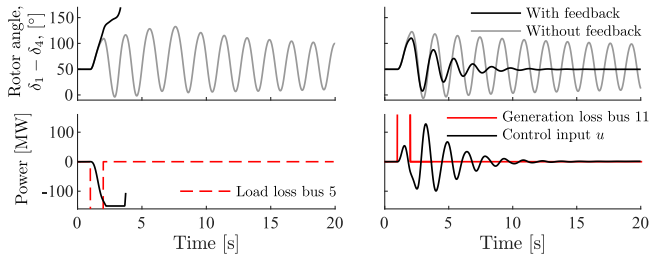


Fig. 9. Rotor phase angles following a 350 MW load/generation disturbance. Feedback control using local voltage phase angle measurement, $y = \theta_9$.

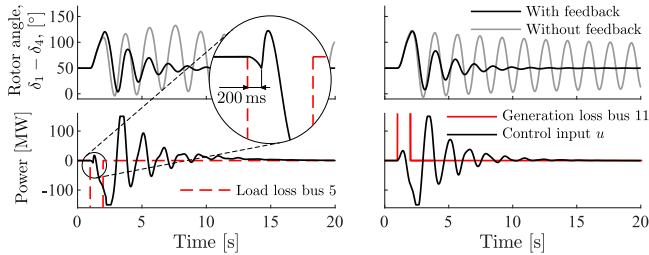


Fig. 10. Rotor phase angle differences following a 350 MW load/generation disturbance. Feedback control using local voltage phase angle measurement and external machine speed measurement, $y = [\theta_9, \omega_1 (200 \text{ ms delay})]^T$.

bus. However for disturbances occurring in the other end of the system, the sensor feedback limitations causes the initial control response to be in the wrong direction. The increased rotor phase angle difference causes a system separation during the first swing.

In this implementation, the input signal has been saturated at ± 160 MW. The transient stability could be improved by reducing this saturation limit or by reducing the feedback gain. However, such changes will affect the resulting damping performance. Another method could be to use alternative or complementary measurements. In Fig. 10, rotor speed measurements ω_1 with a 200 ms communication delay have been added. We see that the new POD controller achieves the same damping ratio without causing transient instability.

VI. CONCLUSIONS

Sensor feedback limitations for POD and transient stability using feedback from local phase angle or frequency measurements has been analyzed. For a linearized two-machine power system modeled it was shown that, although arbitrarily good damping can be achieved, sensor feedback limitation dictates that damping improvement must come at the cost of decreased transient performance. Using a detailed power system model, it was shown that this decrease in transient performance may result in transient instability.

If traditional control methods yields unsatisfactory performance, an engineer may want to try optimization tools to get a better performing control design. An increased understanding of the control problem is valuable as it offers insight into what a good performing control design is and if a more complex control design will be worth the effort.

Local phase angle measurement has been studied since it is commonly used for POD design. In future work this analysis

will be expanded to involve other common measurement signals such as voltage amplitude or ac power flow. The participation of phase angle or frequency deviations in the inter-area mode are relatively easy to understand as they directly reflect the states in the swing equation. Voltage and ac power measurements can be less intuitive and may also be more sensitive to unmodelled dynamics or changing system conditions. However, the sensor feedback limitations shown in this work may be circumvented as they do not apply to voltage or ac power measurements.

REFERENCES

- [1] P. Kundur *et al.*, "Definition and classification of power system stability IEEE/CIGRE joint task force on stability terms and definitions," *IEEE Trans. Power Syst.*, vol. 19, no. 3, pp. 1387–1401, May 2004.
- [2] V. Venkatasubramanian and Y. Li, "Analysis of 1996 Western American Electric Blackouts," in *Proc. Bulk Power System Dynamics and Control-VI*, Cortina d'Ampezzo, Italy, 2004.
- [3] P. Kundur, *Power System Stability and Control*. New York: McGraw-Hill, 1994.
- [4] P. W. Sauer and M. A. Pai, *Power System Dynamics and Stability*. Upper Saddle River, NJ: Prentice hall, 1998, vol. 101.
- [5] P. Kundur, M. Klein, G. J. Rogers, and M. S. Zywno, "Application of power system stabilizers for enhancement of overall system stability," *IEEE Trans. Power Syst.*, vol. 4, no. 2, pp. 614–626, May 1989.
- [6] I. Kamwa *et al.*, "Wide-area monitoring and control at Hydro-Québec: Past, present and future," in *Proc. IEEE/PES General Meeting*, Montréal, Canada, Jun. 2006, pp. 1–12.
- [7] D. Trudnowski, D. Kosterev, and J. Undrill, "PDCI damping control analysis for the western North American power system," in *Proc. IEEE/PES General Meeting*, Vancouver, Canada, Jul. 2013, pp. 1–5.
- [8] J. L. Domínguez-García, F. D. Bianchi, and O. Gomis-Bellmunt, "Control signal selection for damping oscillations with wind power plants based on fundamental limitations," *IEEE Trans. Power Syst.*, vol. 28, no. 4, pp. 4274–4281, Nov. 2013.
- [9] M. A. Elizondo *et al.*, "Interarea oscillation damping control using high voltage dc transmission: A survey," *IEEE Trans. Power Syst.*, vol. 33, no. 6, pp. 6915–6923, Nov. 2018.
- [10] S. Zhang and V. Vittal, "Design of wide-area power system damping controllers resilient to communication failures," *IEEE Trans. on Power Syst.*, vol. 28, no. 4, pp. 4292–4300, Nov. 2013.
- [11] T. Smed and G. Andersson, "Utilizing HVDC to damp power oscillations," *IEEE Trans. Power Del.*, vol. 8, no. 2, pp. 620–627, Apr. 1993.
- [12] L. Harnefors, N. Johansson, and L. Zhang, "Impact on interarea modes of fast HVDC primary frequency control," *IEEE Trans. Power Syst.*, vol. 32, no. 2, pp. 1350–1358, Mar. 2017.
- [13] J. Björk, "Performance quantification of interarea oscillation damping using HVDC," Licentiate Thesis, KTH Royal Institute of Technology, Stockholm, Sweden, 2019.
- [14] J. Björk, K. H. Johansson, and L. Harnefors, "Fundamental performance limitations in utilizing HVDC to damp interarea modes," *IEEE Trans. Power Syst.*, vol. 34, no. 2, pp. 1095–1104, Mar. 2019.
- [15] S. Skogestad and I. Postlethwaite, *Multivariable Feedback Control: Analysis and Design*. New York: Wiley, 2007, vol. 2.
- [16] D. Mondal, A. Chakrabarti, and A. Sengupta, *Power System Small Signal Stability Analysis and Control*. Boston, MA: Academic Press, 2014.
- [17] M. A. Abido, "Optimal design of power-system stabilizers using particle swarm optimization," *IEEE Trans. Energy Convers.*, vol. 17, no. 3, pp. 406–413, Sep. 2002.
- [18] F. Dörfler and F. Bullo, "Kron reduction of graphs with applications to electrical networks," *IEEE Trans. Circuits Syst. I*, vol. 60, no. 1, pp. 150–163, Jan. 2013.
- [19] M. M. Seron, J. H. Braslavsky, and G. C. Goodwin, *Fundamental Limitations in Filtering and Control*. London: Springer, 1997.
- [20] J. S. Freudenberg, C. V. Hollot, R. H. Middleton, and V. Toochinda, "Fundamental design limitations of the general control configuration," *IEEE Trans. Autom. Control*, vol. 48, no. 8, pp. 1355–1370, Aug. 2003.
- [21] I. Kamwa, "Performance of three PSS for interarea oscillations," [Online]. Available: <https://mathworks.com> [Accessed Sep. 24, 2019].